

# PRESSURE EFFECTS ON ALAMETHICIN CONDUCTANCE IN BILAYER MEMBRANES

L. J. BRUNER

*Department of Physics, University of California, Riverside, California 92521*

J. E. HALL

*Department of Physiology and Biophysics, University of California, Irvine, California 92717*

**ABSTRACT** We report here the first observations of the effects of elevated hydrostatic pressure on the kinetics of bilayer membrane conductance induced by the pore-forming antibiotic, alamethicin. Bacterial phosphatidylethanolamine-squalene bilayer membranes were formed by the apposition of lipid monolayers in a vessel capable of sustaining hydrostatic pressures in the range, 0.1–100 MPa (1–1,000 atm). Principal observations were (a) the lifetimes of discrete conductance states were lengthened with increasing pressure, (b) both the onset and decay of alamethicin conductance accompanying application and removal of supra-threshold voltage pulses were slowed with increasing pressure, (c) the onset of alamethicin conductance at elevated pressure became distinctly sigmoidal, suggesting an electrically silent intermediate state of channel assembly, (d) the magnitudes of the discrete conductance levels observed did not change with pressure, and, (e) the voltage threshold for the onset of alamethicin conductance was not altered by pressure. Apparent activation volumes for both the formation and decay of conducting states were positive and of comparable magnitude, namely,  $\sim 100\text{\AA}^3/\text{event}$ . Observation *d* indicates that channel geometry and the kinetics of ion transport through open channels were not affected by pressure in the range employed. The remaining observations indicate that, while the relative positions of free-energy minima characterizing individual conducting states at a given voltage were not modified by pressure, the heights of intervening potential maxima were increased by its application.

## INTRODUCTION

Pressure has been introduced into the study of biological systems at all levels, including intact higher organisms, bacteria, viruses, and proteins. An extensive review of earlier work was provided by Johnson et al. (1974). Evidence of continuing interest is provided by more recent reviews on pressure effects on intact animals (MacDonald et al., 1980), on enzyme mechanisms (Douzou, 1979), on membrane ion transport mechanisms (Péqueux, 1980), and on phase transitions in proteins, nucleic acids, and phospholipids (Heremans, 1982).

Studies of pressure effects at the molecular level generally focus upon effects on reaction rates and equilibria, and are of particular interest because they yield information on volume changes accompanying the reaction. Pressure effects on reaction rates provide information on activation volume,  $\Delta V^\ddagger$ , as described by the equation

$$\Delta V^\ddagger = -k_B T (\partial \ln k / \partial P) \quad (1)$$

where  $k$  is a unidirectional rate constant characterizing a particular reaction step,  $P$  is the pressure,  $k_B$  is Boltzmann's constant, and  $T$  is the absolute temperature. The activation volume,  $\Delta V^\ddagger$ , is interpreted as the extremal volume change accompanying the molecular rearrangements that takes place during the reaction step. Pressure

effects on chemical equilibrium provide information on reaction volumes,  $\Delta V$ , as described by

$$\Delta V = -k_B T (\partial \ln K / \partial P), \quad (2)$$

where  $K$  is an equilibrium constant characterizing a particular reaction. Thus  $\Delta V$  measures a difference in volume between reactant and product states. Activation and reaction volumes can be of either sign. Processes characterized by positive volumes are impeded by pressure and vice versa. In addition to references cited above, any recent review on high-pressure solution chemistry, e.g., Asano and Le Noble (1978) may be consulted for further details.

For this study we selected alamethicin, a pore-forming antibiotic known to form voltage-dependent channels in bilayer membranes. Its structure and properties were described fully in recent reviews (Hall, 1978; Latorre and Alvarez, 1981). It is well established that the conducting unit in alamethicin-doped membranes is an oligomer containing on the order of 10 monomeric units. This clearly represents a more complex situation than, for example, that of gramicidin (Veatch, 1976), where the conducting unit is known to be a dimer. In choosing alamethicin for this initial study we have reasoned that, precisely because of this greater complexity, larger activation and/or reaction volumes would be likely, leading to more readily resolved pressure effects.

## MATERIALS AND METHODS

### Generation of Pressure

Pressures to 100 MPa<sup>1</sup> were generated by the means illustrated in Fig. 1. With vent and bypass valves closed, and all other valves open, the system was pressurized with helium gas to cylinder pressure (10–15 MPa) through a regulator valve. Then the cylinder was isolated and the vent valve was opened to insure against accidental back pressurization of the regulator. Further system pressurization to 100 MPa was accomplished by means of a hand-operated oil pump (model 46-3150; American Instrument Co., Silver Springs, MD). During this phase of operation, oil rising in the high pressure reservoir compressed the gas above it. The volume of this reservoir was sufficient to insure that no oil escaped even at maximum pressure. Further, the cell may be isolated at any pressure by closure of the valve provided for this purpose. Connection between this valve and the cell was provided by a 1.5-m length of coiled high-pressure stainless-steel capillary tubing of inside diameter, 0.5 mm. At the conclusion of a run the system was depressurized by slowly opening the bypass valve and permitting the system pressure to drive the oil back into the ambient pressure reservoir.

### Pressure Cell

A pressure vessel suitable for containment of hydrostatic pressures to 100 MPa, illustrated in Fig. 2, was fabricated from a nonmagnetic stainless steel (type 303). The working volume of the vessel was cylindrical, with a bore and depth of 3.81 cm (1.5 in). Vessel wall thicknesses were 1.90 cm (3/4 in). The vessel was closed by means of an O-ring sealed lid of the same thickness, secured by eight hardened steel bolts (3/8–13 in). The vessel was fitted with ports for introduction of pressurizing gas (He), and for attachment of a bonded silicon strain-gauge pressure transducer (model 2073-7801; LFE Corp., API Instruments Div., Waltham, MA). Finally, the cap of the pressure vessel was fitted with an O-ring sealed threaded port (not shown in Fig. 2) through which alamethicin additions were made by syringe after the vessel was closed and a membrane was formed.

The chamber in which membranes were formed was machined from a block of Teflon (E.I. Du Pont de Nemours & Co. Inc., Wilmington, DE) to fit the interior of the pressure vessel. A Teflon cup with a 0.25-mm membrane aperture was then slipped into the block to complete a two compartment cell. Into each compartment was fitted a Teflon plunger hanging from a screw that in turn formed the lower end of an O-ring sealed rotary feedthrough passing through the lid of the pressure vessel. Each plunger was mounted eccentrically so that, as the feedthrough was rotated from outside the vessel, the plunger was constrained to move up or down depending upon the sense of rotation. In this way the water level in either compartment could be independently raised or lowered past the aperture upon which the membrane was formed. At the bottom of each compartment a Teflon-coated stirring bar was placed that could be driven by a magnet placed beneath the pressure vessel.

Electrical contact to the membrane was provided by Ag/AgCl electrodes not shown in Fig. 2. Spring-loaded contacts to hermetic feedthroughs (type 24916-19501; Astro Seal Inc., South El Monte, CA) completed coaxial connection of the electrodes to external circuitry.

### Membrane Formation

Bilayer membranes were formed by apposition of lipid monolayers as initially described by Montal and Mueller (1972). Bacterial phosphatidylethanolamine (PE) (Avanti Biochemicals, Inc., Birmingham, AL) was dried by evaporation under flowing argon gas of the chloroform solvent in

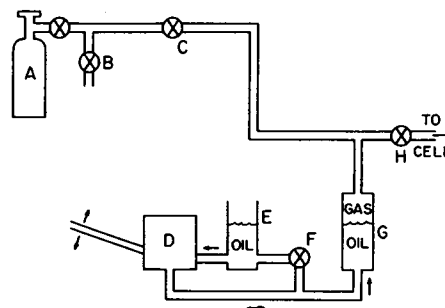


FIGURE 1 Apparatus for the generation of pressure is illustrated. The essential components are as follows. A, gas cylinder with regulator; B, vent valve; C, regulator isolation valve; D, hand-operated pump; E, ambient pressure oil reservoir; F, bypass valve; G, high pressure oil reservoir; H, cell isolation valve.

which it was supplied. Then the lipid was resuspended in pentane at a concentration of 20 mg/ml.

Both squalene (White, 1978) and the lipid/pentane solution were applied to the surfaces of the aqueous solutions that filled the cell to a level ~3-mm below the membrane aperture. The solutions were unbuffered 1.0 M KCl. Then the pressure vessel cap with fully raised plungers attached was bolted into position. The plungers were then lowered successively by a predetermined amount sufficient to raise the liquid levels above the aperture in the Teflon cup. Membrane formation was detected by monitoring the marked increase in interelectrode capacitance that accompanies the process.

### Alamethicin

Natural alamethicin was shown by high-pressure liquid chromatographic separation to consist of at least 12 distinguishably different polypeptides (Balasubramanian, et al., 1981). The structure of the major fraction (fraction 4) was established by synthesis and confirmation of antibiotic activity. This fraction is characterized in the PE model membrane system

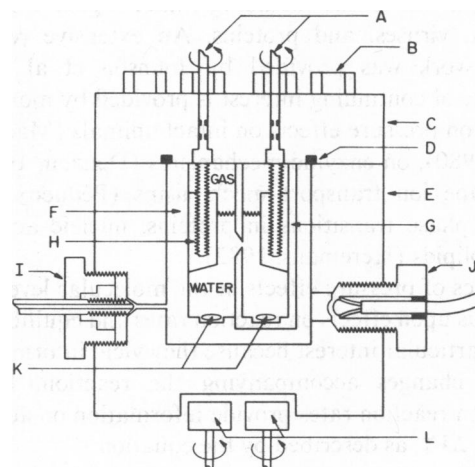


FIGURE 2 The cell for membrane measurements at elevated pressure is illustrated. The essential components are as follows. A, rotary feedthroughs for plunger drive; B, retaining bolts for pressure vessel cap; C, Stainless steel vessel cap; D, O-ring pressure seal; E, stainless steel pressure vessel body; F, Teflon block (membrane cell); G, Teflon cup with membrane aperture; H, plungers for liquid level control; I, high pressure gas inlet; J, silicon strain gauge transducer; K, Teflon-coated stirring bars; L, stirring bar drive magnets; electrodes and electrical feedthroughs are not shown.

<sup>1</sup>The International Union of Pure and Applied Physics recommended unit of pressure, 1 pa (pascal) equals 1N·m<sup>-2</sup>, is used throughout. One standard atmosphere is ~0.1 MPa.

by its ability to produce discrete, well-defined conductance states (Vodyanoy et al., 1982), as exhibited in Fig. 3 *A, B*. This purified major component was used in all the studies described. All references to alamethicin are to the purified major fraction.

## Computer Control and Analysis of Experiments

A computer (system Z2-D; Cromemco Inc., Mountain View, CA) was employed in the conduct of two types of experiments. In the first type, single conductance-state lifetime measurements, membrane current vs. time data as illustrated in Fig. 3 were acquired. To accomplish this, a suitable direct current (dc) voltage was impressed across a membrane incorporated into the input circuit of an operational amplifier (model 3523; Burr-Brown Research Corp., Tucson, AZ) used as a current-to-voltage converter. The operational-amplifier output was further amplified and filtered as required, then passed to an instrumentation tape recorder (model 115; Tandberg Data Inc., San Diego, CA). The resulting data tapes store current vs. time records for subsequent playback to the computer that generates a conductance level histogram as shown in Fig. 4 *A*. The analog-to-digital conversion required was accomplished by use of an eight bit digital-to-analog converter (model MC 1408; Motorola, Inc., Phoenix, AZ) in a successive approximation circuit. After designating the conductance bands appropriate to each resolved conductance state (see Fig. 4 *A*), the operator again played the data tape to the computer. On this second pass, the time duration in each band was measured and stored. The computer program then analyzed the data, generating for each band a lifetime distribution that plotted, as a function of dwell time in the band, the fraction of events persisting for at least that time. Since the ordinate scale was logarithmic (see Fig. 4 *B*), the channel lifetime was simply related to the slope of the corresponding lifetime distribution for the band in question.

The second type of experiment examined the kinetics of the onset and decay of alamethicin conductance accompanying application and removal of supra-threshold transmembrane voltage pulses. Three different pulse protocols were used in kinetics experiments, as illustrated in Fig. 6. Voltage pulses were generated digitally under program control by the computer, then output to the membrane through a digital-to-analog converter (model MC 1408; Motorola, Inc.) and buffer amplifier (model AD514; Analog Devices, Inc., Norwood, MA). For each protocol the operator set pulse amplitude and duration parameters, as well as the parameter increments needed for a complete pulse sequence. The program also permitted repetition of each member of the pulse sequence, with averaging of the accumulated current responses. Current responses were digitized, averaged, and stored on magnetic disks for subsequent display and analysis.

## RESULTS

### Single-Channel Measurements

As noted above, the purified major fraction of alamethicin is known to produce discrete, well-defined conductance states in the bacterial PE model membrane system (Vodyanoy et al., 1982). Membranes formed in the pressure cell exhibit this characteristic in the presence of alamethicin at ambient pressure (Fig. 3 *A*) and at pressures to 100 MPa (Fig. 3 *B*). Comparison of these current vs. time records showed, however, that the conductance state lifetimes were markedly lengthened at elevated pressure. At the same time it is evident from comparison of these records that the conductances of the individual states were not detectably altered in the pressure range accessible with our apparatus. An interesting phenomenon, which we

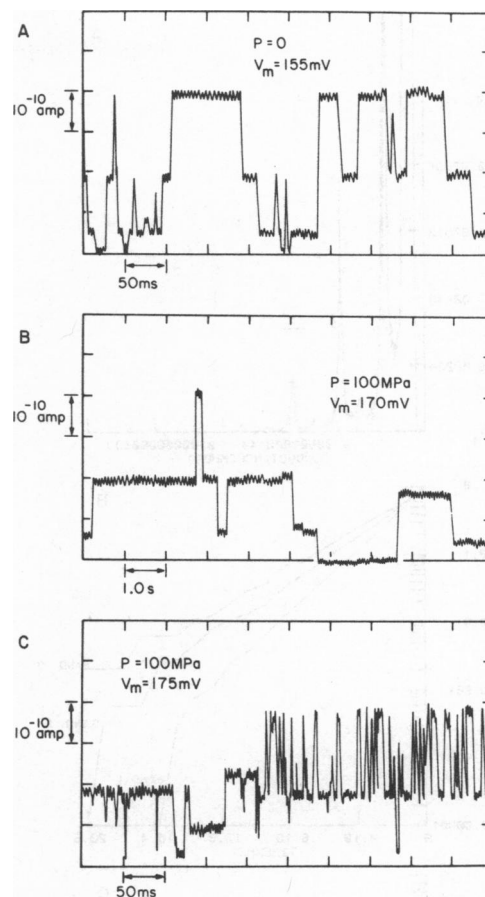


FIGURE 3 Typical recordings of current vs. time with resolved individual conducting states of the alamethicin channel are shown. Alamethicin was added to one compartment only, to a final concentration of  $4 \times 10^{-10}$  gm/ml. (*A*) A current-time record at ambient pressure. (*B*) A similar record at 100 MPa shows a markedly increased conducting state lifetime. Note the change of time scale. (*C*) An example of flicker effect occasionally seen at elevated pressure. Comparison of *A* and *B* shows that the magnitudes of the discrete conductance states are unaltered by pressure. Pooling of data at the same pressure from different runs gives for the highest level illustrated,  $2,800 \pm 300$  pS at ambient pressure, and  $2,900 \pm 300$  pS at 100 MPa. For the intermediate level the corresponding conductances are  $1,250 \pm 200$  pS, and  $1,400 \pm 300$  pS. For the lowest conducting level resolved, the conductance is  $370 \pm 100$  pS at both ambient pressure and 100 MPa.

describe as a "flicker effect," was observed occasionally at the upper end of our pressure range. As illustrated in Fig. 3 *C*, it involves a burst of rapid transitions between adjacent levels that are barely within the time resolution limit (1 ms) of the electronics. Since this effect occurred only at elevated pressure, and then only infrequently, occupying <5% of the time on a typical tape record, we made no systematic study of the phenomenon.

Tape records of current vs. time that illustrate individual conductance states of a single channel were used to generate conductance histograms and lifetime distributions as illustrated in Fig. 4 *A–C*. The procedure is described in the preceding section. Fig. 4 *A, B* illustrate a typical conductance histogram and lifetime distribution generated from

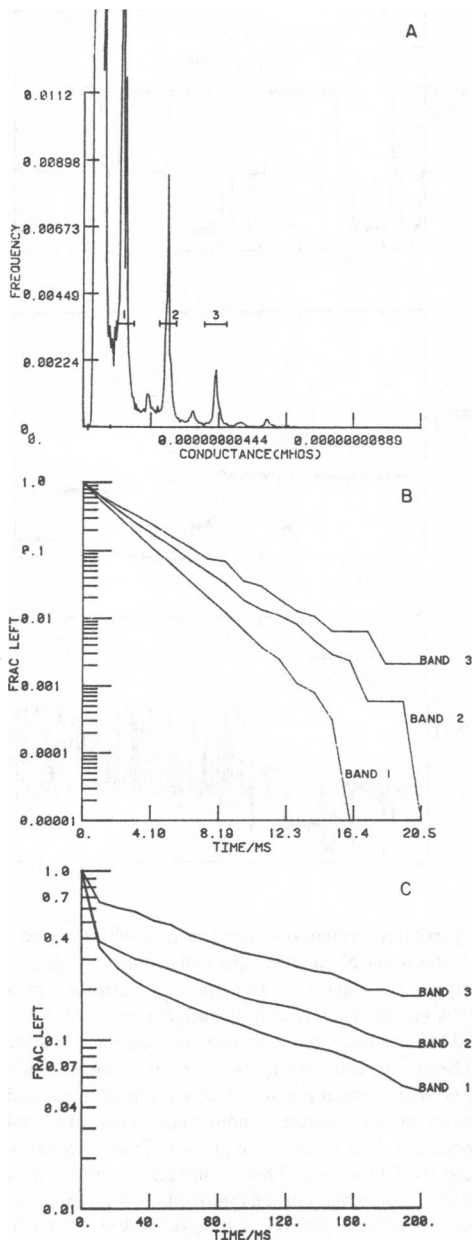


FIGURE 4 Typical analyses of single-level data are illustrated. (A) A current (conductance) histogram is shown with three bands, each encompassing a single level, delineated. (B) A lifetime distribution generated from the same tape record provides a determination of the lifetime of states in each band. For this record, taken at ambient pressure, the alamethicin concentration is  $4 \times 10^{-9}$  gm/ml and the transmembrane voltage is 90 mV. (C) A lifetime distribution taken from a single level record at a pressure of 67 MPa shows a bimodal distribution of relaxation times for the levels in each band, as discussed in the text. For this record the alamethicin concentration is  $10^{-9}$  gm/ml and the transmembrane voltage is 130 mV.

the same data tape recorded at ambient pressure (0.1 MPa). Fig. 4 C illustrates a lifetime distribution generated from single conductance-state data recorded at a pressure of 67 MPa (10,000 PSI). The extended time scale reflects the lengthened lifetime in each level induced by elevated pressure. In this case an early fast decay of the survival

fraction, probably associated with onset of the flicker effect, is evident. Note that, while these fast events occupy a small fraction of a tape record, they will contribute a much larger fraction of the total events recorded on a lifetime distribution because of the large number of events generated during a burst. It is, nevertheless, possible to unambiguously determine a conductance-state lifetime appropriate to the more typical longer-lived events.

The influence of pressure on conductance-state lifetime is illustrated for a single (level) band, Band 2, in Fig. 5. Results for this band at two different transmembrane voltages are shown. Activation volumes appropriate to each of the linear plots are indicated. Similar data were obtained for Bands 1 and 3 as well; all data are presented in Table I.

### Kinetics Measurements

Eisenberg et al. (1973) have shown that, in the presence of many conducting pores, their average number,  $\bar{n}$ , can be well represented by a first-order differential equation

$$\frac{d\bar{n}}{dt} = \mu - \lambda\bar{n}. \quad (3)$$

Membrane conductance is proportional to  $\bar{n}$ . The parameter  $\mu$  is an exponentially increasing function of forward voltage, while  $\lambda$  decreases exponentially with voltage. To establish the pressure dependence of these parameters as well, we used the voltage-pulse protocols illustrated in Fig. 6. In any given experiment, the parameter  $\mu$  can be measured over a narrow range of voltage by applying a pulse sequence as illustrated in Fig. 6 A. Ideally, the pulse duration should be long enough to permit an approach to steady state. The pulse amplitude was incrementally

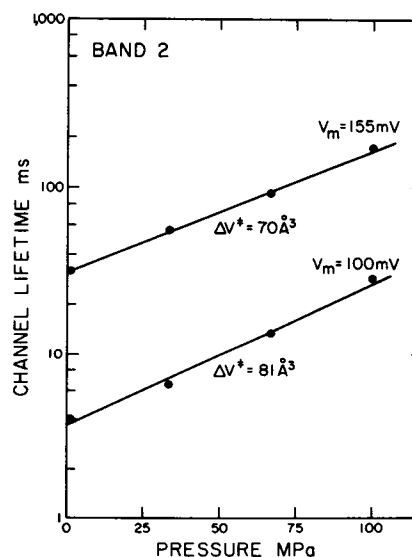


FIGURE 5 A semi-log plot of level lifetime vs. pressure is presented for Band 2 at two different transmembrane voltages. The activation volume is given for each case.

TABLE I  
ACTIVATION VOLUMES CHARACTERISTIC OF  
DISCRETE CONDUCTANCE STATES OF THE  
ALAMETHICIN CHANNEL

Band	Transmembrane voltage	
	100 mV	155 mV
1	76	56
2	81	70
3	75	70

decreased and the current response was measured at each amplitude. The maximum slope of each current vs. time curve provided a measure of  $\mu(V_m, P)$ .

The measurement of  $\lambda(0, P)$  was accomplished by detecting the current response to double-pulse sequences, as illustrated in Fig. 6 B. In this case the interpulse delay was incrementally increased. The ratio of the conductance at the beginning of the second pulse to that at the end of the first provided a measure of the fractional decay of open pores during the interpulse period, over which  $V_m = 0$ . The decay was dominated by the second term on the right of Eq. 3 during this period.

Finally, to obtain  $\lambda(V_m, P)$  for  $V_m \neq 0$ , we used a "stepdown" sequence such as illustrated in Fig. 6 C. Again the rate of decay of current following voltage stepdown was generally dominated by the second term on the right of Eq. 3. Since the steady state solution of Eq. 3 is,  $\bar{n} = \mu/\lambda$ , the reduction in steady state level following voltage step down provides a ready measure of the shift in relative amplitude of these terms.

In Fig. 7 A, B we illustrate typical current responses, at

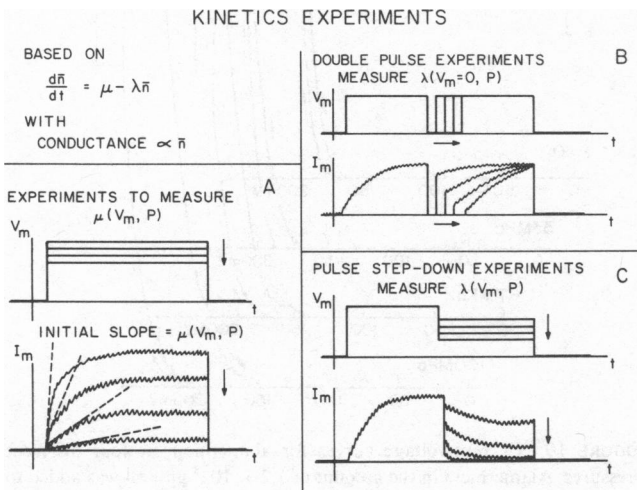


FIGURE 6 Voltage pulse protocols used for the determination of kinetic parameters are illustrated. (A) Pulse sequence used to determine  $\mu$  as a function of transmembrane voltage and of pressure. (B) Double pulse sequence used to determine  $\lambda$  as a function of pressure at zero transmembrane voltage. (C) Pulse step-down sequence used to determine  $\lambda$  as a function of pressure at subthreshold transmembrane voltages different from zero.

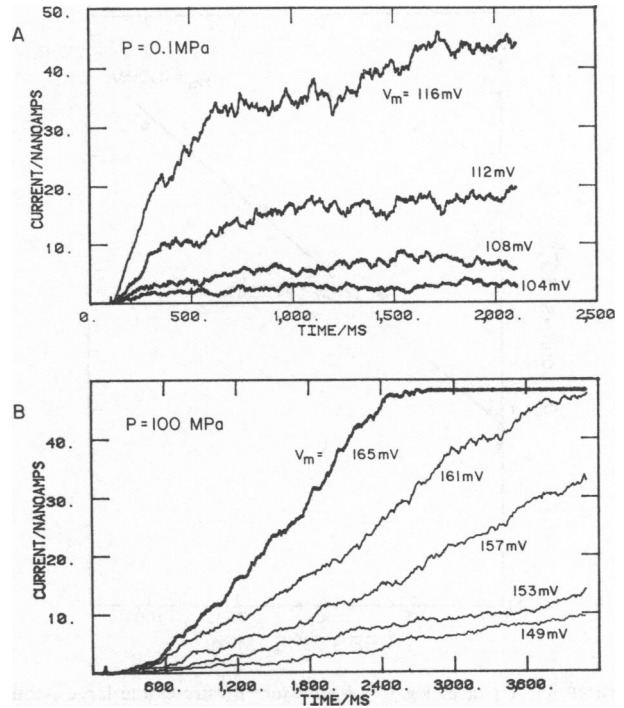


FIGURE 7 Representative current responses to voltage pulse sequences of the type depicted in Fig. 6 A are shown. Each curve is the average of four applications of the same pulse amplitude. In each case  $4 \times 10^{-8}$  gm/ml of alamethicin was added to the aqueous phase on one side only of the membrane. (A) The current response at an ambient pressure of 0.1 MPa is shown. (B) The much slower and distinctly sigmoidal current response at an elevated pressure of 100 MPa is shown. The capacitive current spike at  $t = 100$  ms indicates the point of application of the voltage pulse in each case.

ambient pressure and at 100 MPa, respectively, to voltage-pulse sequences as illustrated in Fig. 6 A. It is evident that the rate of increase of current (conductance) was markedly slowed at elevated pressure. In fact, no steady state was reached during the pulse interval chosen. In addition, a distinctly sigmoidal "turn-on" of the membrane current was seen at 100 MPa. The maximum rate of increase of current was taken as a measure of  $\mu$  in this case. A plot of  $\log \mu^{-1}$  vs.  $P$  is shown in Fig. 8 for a transmembrane voltage of 100 mV. The marked positive slope, from which a positive activation volume of  $150 \text{ \AA}^3$  can be inferred, reflects the inhibition by pressure of the pore-formation process.

Fig. 9 shows plots of  $\log \lambda^{-1}$  vs. pressure at transmembrane voltages of zero and 100 mV, obtained by the protocols of Fig. 6 B, C, respectively. It is seen that  $\lambda^{-1}$  decreases with decreasing  $V_m$  at fixed pressure, and that  $\lambda^{-1}$  increases with pressure, giving the positive activation volumes shown for each plot. Since  $\lambda^{-1}$  measures the mean time required for the conducting state of the membrane to disappear, a comparison with the single conducting state lifetime data of Fig. 5, and of Table I, is appropriate. Upon direct comparison at  $V_m = 100$  mV, we noted that, at any given pressure,  $\lambda^{-1}$  values were larger than single-level

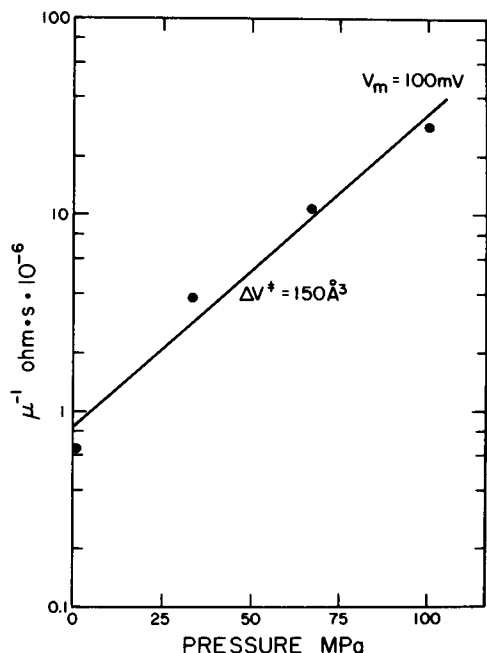


FIGURE 8 A plot of  $\log \mu^{-1}$  vs. pressure illustrates the large positive activation volume characteristic of the process of conducting pore formation.

lifetimes by about an order of magnitude. In addition, the activation volume characteristic of  $\lambda^{-1}$  was lower by about a factor of two.<sup>2</sup> In considering these differences note that the measurement of  $\lambda^{-1}$  involves much higher magnitudes of conductance than does the measurement of single-level lifetimes. A much higher density of conducting entities or pores, opened on average to higher conductance levels, is expected. The shutdown of this higher order conductance must involve a stepwise downward cascade through multiple individual conducting states of the channels.

### Current-Voltage Characteristics

In this study we have sought to determine the effect of pressure on the steady state current-voltage (I-V) characteristics of alamethicin-doped membranes, in particular, on the threshold voltage for the onset of conductance. Because there is a normal tendency for the threshold voltage to drift upward with time after alamethicin addition, we waited for 3 h after addition to commence the run that produced the data shown in Fig. 10. All four of the I-V curves shown were taken at the same sweep rate of 3 mV/s, and all showed hysteresis, which became much more prominent as the pressure was increased. This opening up of the I-V curves was expected, in view of the fact that pressure slows the approach to equilibrium (Fig. 7).

<sup>2</sup>This result could be attributed to possibly lower activation volumes characteristic of transitions between higher conductance levels of the channels, not observed in the single-level lifetime measurements. Interactive effects between channels could also be involved.

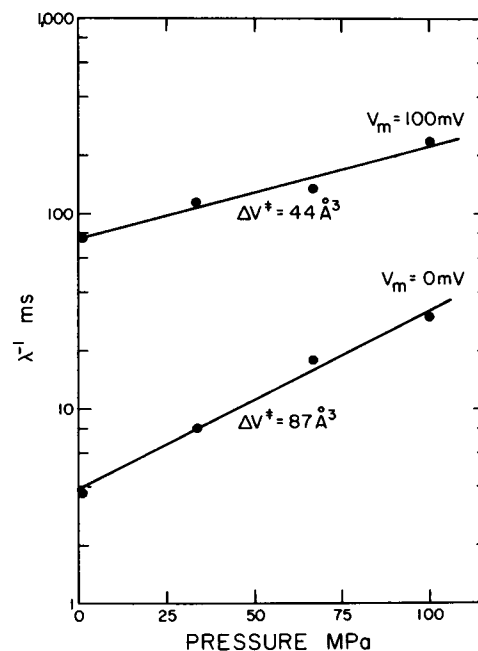


FIGURE 9 Plots of  $\log \lambda^{-1}$  vs. pressure, at two different transmembrane voltages, reveal positive activation volumes characteristic of the decay of higher order conductance.

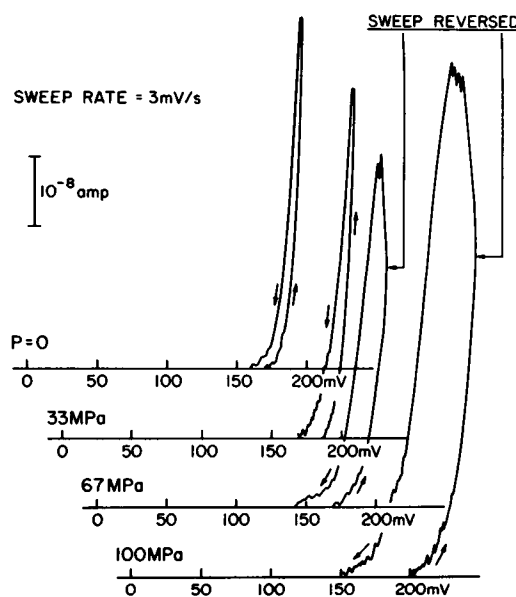


FIGURE 10 Current-voltage curves for alamethicin at four different pressures. Alamethicin in the amount of  $1.2 \times 10^{-8}$  gm/ml was added to the aqueous phase on one side of the membrane. Using a fixed sweep rate of 3 mV/s, we observed a progressive increase of hysteresis with pressure. We adopted as a measure of the steady state I-V curve the mean of the two voltages corresponding to each level of current, and defined the voltage threshold as done previously (Eisenberg et al., 1973). In this way we determine a voltage threshold of  $175 \pm 10$  mV for each pressure. We conclude that the voltage threshold for the onset of alamethicin conductance is insensitive to pressure to 100 MPa.

Inspection of Fig. 10, making due allowance for hysteresis, indicates that the voltage threshold for the onset of conductance was not significantly affected by pressure.

## DISCUSSION

We summarize first the effects of pressure on alamethicin conductance. They are (a) the application of pressure markedly lengthened single conductance-state lifetimes, (b) the magnitudes of the conductances contributed by discrete conductance states were not influenced by pressure, (c) both the onset and decay of higher level alamethicin conductance were slowed by pressure, (d) the onset of alamethicin conductance became distinctly sigmoidal at elevated pressure, and (e) the threshold voltage for the onset of alamethicin conductance was insensitive to pressure.

Observation *b* above suggests that the geometry of conducting pores is not modified appreciably by applied pressure in the range employed here. At 25°C the viscosity of bulk water changes by no more than 2% as pressure increased from ambient to 100 MPa (Bett and Cappi, 1965). Comparably small variations with pressure of aqueous electrolyte conductivity are also observed (Hamann, 1974). Thus our data are consistent with the view that the conductance of a given state is governed by the geometry of a pore filled with aqueous electrolyte having a conductivity comparable to that of the surrounding bulk solutions. In this view neither the geometry of the open pore nor the conductivity of the medium that fills it is sensitive to pressures to 100 MPa.

Observations *a* and *c* above indicate that both the formation and the destruction of conducting states were impeded by elevation of pressure. We considered the possibility that both processes were diffusion-controlled, i.e., involve a rate limiting diffusive step. Since the viscosity of water at 25°C is insensitive to pressure as mentioned above, it is unlikely that diffusion through the aqueous phase would be involved. Studies of the pressure dependence of self-diffusion in liquid *n*-alkanes, however, (McCall et al., 1959) reveal positive activation volumes amounting to 10–15% of the molar volume of the species in question. A simple extrapolation of these results to the alamethicin monomer, with a molecular weight of 1,600 and a molecular volume of roughly 1,800 Å<sup>3</sup>, would indicate a positive activation volume of ~200 Å<sup>3</sup>. This value should undoubtedly be regarded as an upper limit. Data on activation volumes for diffusion of longer chain organic molecules through a molten polymer matrix (Rennie and Tabor, 1980) suggest that diffusion occurs by motion of segments of the carbon backbone only, with upper limiting activation volumes of 70–80 Å<sup>3</sup>. It is evident that, with respect to both the sign and magnitude of the activation volume for formation and decay of conducting states, our observations are consistent with rate limiting by a diffusion-controlled mechanism.

Three additional points suggest, however, that this view

is oversimplified, particularly with respect to the formation of conducting states. First, the conductance due to alamethicin is strongly voltage-dependent. Second, greater complexity of the formation process is evidenced by observation *d* above, to the effect that the onset of alamethicin conductance becomes sigmoidal at elevated pressure. Finally, the activation volume for  $\mu^{-1}$ , the rate parameter governing the onset of conductance, is larger at a given voltage by at least a factor of two than the activation volumes for either single-level lifetimes or for the rate parameter,  $\lambda^{-1}$ , governing the rate of decay of higher order currents.

It is possible to qualitatively explain this greater complexity of the channel formation process if it is assumed that there exists an electrically silent intermediate state of alamethicin incorporation into the membrane. Such a state has been postulated by previous investigators (Baumann and Mueller, 1974; Boheim, 1974). Monomers must pass through this preassembly state before their assembly into a conducting oligomer can take place. Entry into this postulated preassembly state is driven by the electric field applied across the membrane, and quite likely involves a reorientation of the intrinsic dipole moment of the alamethicin molecule (Schwarz and Savko, 1982; Vodyanoy et al., 1983; Yantorno et al., 1982). A substantial conformational change of the monomer accompanying this reorientation could account for the larger activation volume for the rate parameter,  $\mu^{-1}$ .

The structure of alamethicin in a crystal has recently been deduced by x-ray analysis (Fox and Richards, 1982). The structure does not provide a detailed molecular interpretation for the activation volumes we observed, but there are some suggestive features. In the x-ray structure, residues one through fourteen form an  $\alpha$ -helix. If two  $\alpha$ -helical monomers are placed side-by-side, there is excellent complementarity between the faces of adjacent helices. A striking feature of the contact faces is the regular alternation of bumps and grooves in passing from COOH terminus to NH<sub>2</sub> terminus. The bumps on one monomer can be made to fit into grooves on an adjacent monomer and a fairly reasonable decameric channel model constructed. Using Corey-Pauling-Koltun (CPK) molecular models, we estimated the volume of a single groove to be from 20 to 40 Å<sup>3</sup>. There are about three grooves on one side of the  $\alpha$  helical segment of one monomer. The empty volume of these grooves is thus of the same order of magnitude as the activation volumes we observed. It is thus possible that the transition volume between single-channel states may involve sliding of monomers over one another so the empty groove volume cannot be filled either by bumps on an adjoining molecule or by hydrocarbon chains of the lipid during the transition. It thus appears that the activation volume we observed may have a structural interpretation, and may be consistent with activation volumes observed for diffusion in alkanes. Our data do not allow us to distinguish between these possibilities at present.

All the points considered above may be summarized by reference to Fig. 11 *A, B*, where we present qualitative illustrations of the effects of both voltage and pressure on the free energy of the configuration of the monomer in the membrane. State *S* represents a surface state in which the monomer would normally find itself in the absence of applied transmembrane voltage. State *P* is a postulated nonconducting preassembly state, which becomes much more favorable relative to *S* when a threshold voltage for the onset of alamethicin conductance is applied (Fig. 11 *B*). States 1, 2, 3, etc., represent conducting states, in order of increasing conductance, into which the alamethicin monomer may become incorporated. The additional effect of pressure on the configurational free-energy diagram of Fig. 11 *B* is depicted by the dashed-line curve. Note that pressure slows the rates of transition between all states, but a greater effect on the rates of transition between states *S* and *P* is illustrated. So long as equilibration between states *S* and *P* is rapid compared with that between *P* and the conducting states 1, 2, 3, etc., no sigmoidal increase of current upon application of a supra-threshold voltage pulse would be expected. Should these rates become comparable, however, as would be the case for the dashed-line curve illustrating the effect of pressure, then a sigmoidal increase of current would occur. A greater effect on the potential maximum separating states *S* and *P*

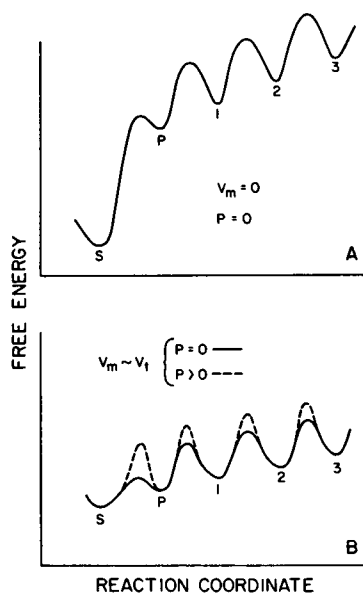


FIGURE 11 The free energy of the alamethicin monomer, as a function of the various membrane configurations available to it, is illustrated qualitatively. State *S* is a nonconducting surface state of the monomer, where it would normally be found at zero transmembrane voltage. State *P* is a nonconducting preassembly state that is made more favorable relative to *S* by applied forward voltage. States 1, 2, 3, etc., are discrete conductance states into which the monomer can be incorporated. (*A*) The configuration diagram at zero voltage and pressure is sketched. (*B*) The configuration diagram at an applied voltage near  $V_1$ , the threshold voltage, is illustrated. The dashed lines (---) depict the additional effect of pressure.

than on the other maxima, as illustrated in Fig. 11 *B*, would clearly promote pressure-dependent sigmoidal current response. The larger activation volume observed for the rate parameter,  $\mu^{-1}$ , supports the view that such a differential-pressure effect actually does occur. In relating these considerations to the experiments note that the turning-on of alamethicin current ( $\mu^{-1}$  measurements) involves transitions  $S \rightarrow P \rightarrow 1, 2, 3$ , etc. Hence transitions between *S* and *P* can be rate limiting. The turning-off of current, on the other hand, requires transitions out of the numbered states into state *P* only. The rate of subsequent transitions into state *S* cannot influence the  $\lambda^{-1}$  measurements. It is for these reasons that the asymmetry of activation volumes characteristic of  $\mu^{-1}$  and of  $\lambda^{-1}$  is observable.

Finally, we note that Fig. 11 *B* has been drawn so as to imply that there is no pressure effect on the relative disposition of the potential minima representing the various possible configurations of the alamethicin monomer. An equivalent statement is that the reaction volumes for the processes accompanying the onset of conductance are negligible. This feature of the configuration diagram is presumed to be influenced by transmembrane voltage only. These conclusions are based on observation *e* above, namely, that the threshold voltage for the onset of alamethicin conductance was insensitive to pressure. Further support is provided by observation *b*, which led us to conclude that pore geometry was unaffected by pressure.

Since helium gas was used as a pressure-transmitting medium in these experiments, we considered whether the observed effects on alamethicin conductance were due to hydrostatic pressure alone, or whether dissolution of the inert gas in the membrane could be a contributing factor. It is well known that other inert gases, such as nitrogen, can produce narcosis in animals and in man under hyperbaric conditions (Miller, 1974), and that this effect can be ameliorated by purely hydraulic compression (animal experiments) or by replacement of nitrogen by helium in the hyperbaric breathing mixture (animals and man). Pressure reversal of inert gas narcosis is generally explained in terms of the "critical volume" hypothesis, which attributes anesthesia to expansion by dissolved gas of hydrophobic membrane sites, this expansion being reversed by purely hydrostatic pressure. Where comparative data are available, it is found that the solubility of helium in hydrocarbon fluids is about an order of magnitude lower than that of nitrogen (Hildebrand et al., 1970). This correlates well with the absence of helium-induced narcosis, as noted above. A further convincing indication of the near equivalence of helium pressure and hydraulic pressure is provided by the spin-probe study of Finch and Kiesow (1979) who showed that pressurization by the two methods produced identical effects on the order parameter at different depths in the membrane, as revealed by the spin probe used. Pressurization by nitrogen, on the other hand, resulted in a significant lowering of the order



parameter. Finally, MacNaughtan and MacDonald (1980) have compared hydrostatic (oil) and hyperbaric gas pressure effects on the phase transition temperature,  $T_m$ , of dipalmitoyl phosphatidylcholine multilamellar liposomes. Comparing hydrostatic, He, and  $N_2$  pressurization, they found values of  $(dT_m/dP)$  of 0.024, 0.021, and 0.006°C/atm, respectively. While these investigators concluded that the fluidizing effects of He and of  $N_2$  would be comparable at the same concentration in the membrane, the concentration of  $N_2$  would be roughly five times greater than that of He at the same pressure because of the lower solubility coefficient of the latter. Since a gas-monolayer-water interface must be present in our experiments, and in view of the evidence cited above, clearly helium is the pressure transmitting medium of choice.

This work was carried out while Dr. Bruner was a visitor in Dr. Hall's laboratory. Dr. Bruner wishes to express appreciation to Dr. Hall and to members of his group, in particular to Dr. I. Vodyanoy, for courtesies extended during this visit.

We are grateful for support provided by National Science Foundation grant PCM-7926672, awarded to Dr. Bruner, and by National Institutes of Health grant HL-23183, awarded to Dr. Hall. Partial support from intramural research funds provided by the University of California is also acknowledged.

Received for publication 9 November 1982 and in final form 25 May 1983.

## REFERENCES

- Asano, T., and W. J. Le Noble. 1978. Activation and reaction volumes in solution. *Chem. Rev.* 78:407-489.
- Balasubramanian, T. M., N. C. E. Kendrick, M. Taylor, G. R. Marshall, J. E. Hall, I. Vodyanoy, and F. Reusser. 1981. Synthesis and characterization of the major component of alamethicin. *J. Am. Chem. Soc.* 103:6127-6132.
- Baumann, G., and P. Mueller. 1974. A molecular model of membrane excitability. *J. Supramol. Struct.* 2:538-557.
- Bett, K. E., and J. B. Cappi. 1965. Effect of pressure on the viscosity of water. *Nature (Lond.)* 207:620-621.
- Boheim, G. 1974. Statistical analysis of alamethicin channels in black lipid membranes. *J. Membr. Biol.* 19:277-303.
- Douzou, P. 1979. The study of enzyme mechanisms by a combination of cosolvent, low-temperature and high-pressure techniques. *Q. Rev. Biophys.* 12:521-569.
- Eisenberg, M., J. E. Hall, and C. A. Mead. 1973. The nature of the voltage-dependent conductance induced by alamethicin in black lipid membranes. *J. Membr. Biol.* 14:143-176.
- Finch, E. D., and L. A. Kiesow. 1979. Pressure, anesthetics, and membrane structure: a spin-probe study. *Undersea Biomed. Res.* 6:41-45.
- Fox, R. O., and F. M. Richards. 1982. A voltage-gated ion channel model inferred from the crystal structure of alamethicin at 1.5-Å resolution. *Nature (Lond.)* 300:325-330.
- Hall, J. E. 1978. Channels in black lipid films. In *Membrane Transport in Biology. Concepts and Models*. G. Giebisch, D. C. Tosteson, and H. Ussing, editors. Springer-Verlag, Berlin. 1:475-531.
- Hamann, S. D. 1974. Electrolyte solutions at high pressure. *Mod. Aspects Electrochem.* 9:47-158.
- Heremans, K. 1982. High pressure effects on proteins and other biomolecules. *Annu. Rev. Biophys. Bioeng.* 11:1-21.
- Hildebrand, J. H., J. M. Prausnitz, and R. L. Scott. 1970. *Regular and Related Solutions*. Van Nostrand Reinhold Company, New York. 201-202.
- Johnson, F. H., H. Eyring, and B. J. Stover. 1974. *The Theory of Rate Processes in Biology and Medicine*. Van Nostrand Reinhold Company, New York. 273-369.
- Läuger, P., and G. Stark. 1970. Kinetics of carrier-mediated ion transport across lipid bilayer membranes. *Biochim. Biophys. Acta.* 211:458-466.
- Latorre, R., and O. Alvarez. 1981. Voltage-dependent channels in planar lipid bilayer membranes. *Physiol. Rev.* 61:77-150.
- MacDonald, A. G., I. Gilchrist, K. T. Wann, and A. E. Wilcock. 1980. The tolerance of animals to pressure. In *Animals and Environmental Fitness*. R. Gilles, editor. Pergamon Press, Oxford. 1:385-403.
- MacNaughtan, W., and A. G. MacDonald. 1980. Effects of gaseous anesthetics and inert gases on the phase transition in smectic mesophases of dipalmitoyl phosphatidylcholine. *Biochim. Biophys. Acta.* 597:193-198.
- McCall, D. W., D. C. Douglass, and E. W. Anderson. 1959. Self-diffusion in liquids: paraffin hydrocarbons. *Phys. Fluids.* 2:87-91.
- Miller, K. W. 1974. Inert gas narcosis, the high pressure neurological syndrome, and the critical volume hypothesis. *Science (Wash. DC)* 185:867-869.
- Montal, M., and P. Mueller. 1972. Formation of bimolecular membranes from lipid monolayers and a study of their electrical properties. *Proc. Natl. Acad. Sci. USA.* 69:3561-3566.
- Péqueux, A. 1980. Osmoregulation and ion transport at high hydrostatic pressure. In *Animals and Environmental Fitness*. R. Gilles, editor. Pergamon Press, Oxford. 1:405-425.
- Rennie, A. R., and D. Tabor. 1980. Hydrostatic pressure and long-chain organic molecule diffusion through a polymer matrix. *Nature (Lond.)* 286:372-373.
- Schwarz, G., and P. Savko. 1982. Structural and dipolar properties of the voltage-dependent pore former alamethicin in octanol/dioxane. *Biophys. J.* 39:211-219.
- Veatch, W. 1976. The structure of the gramicidin A transmembrane channel. *J. Supramol. Struct.* 5:431-451.
- Vodyanoy, I., J. E. Hall, T. M. Balasubramanian, and G. Marshall. 1982. Two purified fractions of alamethicin have different conductance properties. *Biochim. Biophys. Acta.* 684:53-58.
- Vodyanoy, I., J. E. Hall, and T. M. Balasubramanian. 1983. Alamethicin-induced current-voltage curve asymmetry in lipid bilayers. *Biophys. J.* 42:71-82.
- White, S. H., 1978. Formation of "solvent free" black lipid bilayer membranes from glycerol monooleate dispersed in squalene. *Biophys. J.* 23:337-347.
- Yantorno, R., S. Takashima, and P. Mueller. 1982. Dipole moment of alamethicin as related to voltage-dependent conductance in lipid bilayers. *Biophys. J.* 38:105-110.